The impact of carbon materials on the hydrogen storage properties of light metal hydrides

Philipp Adelhelm[*a] and Petra E. de Jongh[b]

The safe and efficient storage of hydrogen is still one of the remaining challenges towards fuel cell powered cars. Metal hydrides are a promising class of materials as they allow the storage of large amounts of hydrogen in a small volume at room temperature and low pressures. However, usually the kinetics of hydrogen release and uptake and the thermodynamic properties do not satisfy the requirements for practical applications. Therefore current research focuses on catalysis and the thermodynamic tailoring of metal hydride systems. Surprisingly, carbon materials used as additive or support are very effective to improve the hydrogen storage properties of metal hydrides allowing fast kinetics and even a change in the thermodynamic properties. Even though the underlying mechanisms are not always well understood, the beneficial effect is probably related to the peculiar structure of the carbon materials. This feature article gives an introduction to the different carbon materials, an overview of the preparation strategies to synthesize carbon/hydride nanocomposites, and highlights the beneficial effect of carbon by discussing two important hydrides: MgH_2 and $NaAlH_4$.

1. Introduction

The use of hydrogen as an energy carrier in the transportation sector holds great prospects in order to reduce CO_2 emissions and the dependency on fossil fuels. For a medium-sized, fuel cell powered car, only around 4 kg of H_2 would be needed to reach a driving range of 400 km.[1] However, due to the peculiarities of hydrogen, the development of a suitable tank system is very challenging. The use of metal hydrides for the solid state storage of hydrogen is promising mainly because they allow the storage of large amounts of hydrogen at low H_2 pressures in a small volume. The hydrogen content of magnesium hydride is 7.7 wt% with a hydrogen density of 110 g L^{-1}, for example (i.e. a MgH_2 block of 52 kg and 36 L contains 4 kg of hydrogen). The concept of a metal hydride tank system in combination with a fuel cell is illustrated in Fig. 1.

However, the requirements for an actual on-board tank system are plenty and so far no metal hydride system is known that could be applied in practice.[2] Currently, the main issues are *thermodynamic* and *kinetic limitations*.

As the waste heat of a PEM fuel cell should be used to sustain the dehydrogenation reaction of the metal hydride, a suitable metal hydride system should exhibit an enthalpy of formation of $\Delta H = -10$ to -40 kJ mol^{-1} H_2, corresponding to an H_2 equilibrium pressure of a few bars during operational conditions (the entropy of the reaction is around 130 J K^{-1} per mol H_2 for all

[a]Institute of Physical Chemistry, Justus-Liebig-University Giessen, Heinrich-Buff-Ring 58, 35392 Giessen, Germany. E-mail: philipp.adelhelm@uni-giessen.de

[b]Inorganic Chemistry and Catalysis, Debye Institute for Nanomaterials Science, Utrecht University, Sorbonnelaan 16, 3584 CA Utrecht, The Netherlands. E-mail: p.e.dejongh@uu.nl

Philipp Adelhelm studied materials science at the University of Stuttgart and conducted his PhD at the Max-Planck-Institute of Colloids and Interfaces in Potsdam (Prof. Antonietti). After receiving his PhD in 2007, he joined the group of Petra de Jongh at Utrecht University as a postdoctoral fellow. Currently he is starting up a junior research group at the University of Giessen in the group of Prof. Janek. His research interests are the preparation and characterization of nanomaterials for hydrogen storage and battery technology.

Philipp Adelhelm

Petra de Jongh received her PhD in photoelectrochemistry in 1999, and worked 5 years as a senior scientist at Philips Research. She is now associate professor at Utrecht University, where she (co)-supervises researchers working on supported nanoparticles, especially for applications in catalysis and energy storage and conversion.
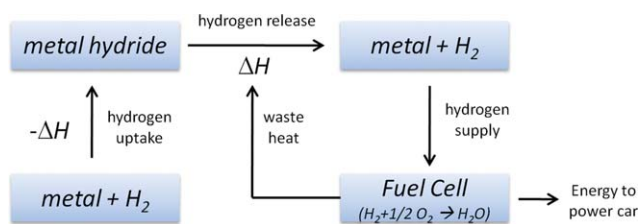
Petra E. de Jongh

Fig. 1 Principle of a metal hydride tank for the reversible storage of hydrogen. Hydrogen is stored by reaction with a metal to form a hydride (exothermic reaction). On demand, the hydrogen is released from the hydride (endothermic reaction), utilizing the waste heat of the fuel cell.

metal hydride systems if the entropies of the non-gaseous phases are neglected). A few metal hydrides fulfill this requirement a priori, e.g. $LaNi_5H_6$ (1.4 wt% H) or $FeTiH_2$ (1.9 wt% H), however their hydrogen contents are too small for mobile applications. Metal hydride systems with higher gravimetric densities, namely light metal hydrides or complex hydrides, are usually too stable (e.g. MgH_2 with $\Delta H = -75$ kJ mol^{-1} H$_2$, 7.7 wt% H) or too unstable (e.g. AlH_3 with $\Delta H = -7.6$ kJ mol^{-1} H$_2$, 10.1 wt% H).

The reactions of hydrogen release und uptake should be fast to allow quick refilling of the tank and sufficient H$_2$ supply of the fuel cell. Current research efforts therefore focus on the improvement of the kinetic behavior and the thermodynamic tailoring of metal hydride systems. Recent approaches include the synthesis of nanostructured composite materials, consisting of a metal hydride phase and an additional phase such as carbon nanotubes, for example. It is believed that by nanosizing, kinetic limitations can be minimized and the thermodynamic stability of the metal hydride system can be modified by size effects or interaction with the additional phase.[3–5] DFT calculations on MgH_2 confined in carbon nanotubes suggest a decrease in ΔH by 50%, for example.[3]

The three main methods to prepare nanocomposites of metal hydrides are shown in Fig. 2. In ball-milling, a phase is dispersed in the hydride phase, whereas infiltration or impregnation of a porous phase (support) usually lead to a finely dispersed hydride phase.[6]

In both cases, the hydrogen storage properties are improved. Faster hydrogen diffusion is aided by the smaller crystallite size or transport along the other phase. Chemical anchoring or confinement of the metal (hydride) by the additional phase can also suppress the undesired crystal growth that is usually observed for nanomaterials upon cycling. On the other hand, the additional phase adds to the effective weight and volume of the tank system, so its use is only feasible for metal hydrides with relatively high H contents.

An important question is therefore which material is most suitable as additive/support for metal hydrides. Classical catalysts (transition metals) are effective but can only be used in small fractions, as they are heavy and usually expensive. A structural additive or a support/scaffold comprises a much larger fraction of the composite material so only light and low cost materials can be used. In this respect, carbon materials are outstanding as they are light, relatively inert and often abundant. An exciting property of carbon is its ability to bond with itself (and other atoms) with different hybridizations, giving rise to allotropes of

completely different properties. Besides the allotropes, plenty carbon materials exist that offer a wide range of interesting properties. Furthermore, carbon is an efficient heat conductor, which is beneficial to the heat transport during hydride formation and decomposition.

In recent years, carbon materials were reported to lead to improvement in kinetics and thermodynamics of hydrogen sorption for different metal hydride systems. An exciting example for the impact on the kinetics of the hydrogen release is sodium alanate ($NaAlH_4$) 2–10 nm particles deposited on carbon nanofibers, with a decrease in activation energy for the first hydrogen release step from 116 kJ mol^{-1} for bulk to 58 kJ mol^{-1}.[7] Also mixing carbon materials and metal hydrides by high-energy ball-milling (or even simple mixing) improves the hydrogen sorption properties.

The recent developments pinpoint the important role of carbon in the development of new metal hydride based hydrogen storage materials. This review starts with the synthesis and structure of carbon materials, and the background of their possible effects on the hydrogen sorption properties of metal hydrides. Then an overview of the preparation techniques of metal hydride/carbon nanocomposites is given. The strong impact of carbon on the kinetics and thermodynamics of metal hydrides is highlighted for two important systems: MgH_2 and $NaAlH_4$. The review will end with a summary on the opportunities and challenges in this field.

2. What carbon materials can be used?

To identify the carbon materials that are most suitable as additive/support for metal hydrides, an exact knowledge of their composition and microstructure is desirable. Carbon materials are widely used in industry in form of e.g. porous powders, fibers, fabrics, pellets, extrudates or composites for very different purposes. This is because carbon materials exhibit, depending on their structure, very different properties. For example, diamond (100% sp^3) is used as abrasive due to its hardness and is electronically insulating. In contrast, graphite (100% sp^2) is very soft and can be used as dry lubricant or as conducting agent. Most of the carbon materials used are non-crystalline and are so-called turbostratic (or non-graphitic) carbons. Compared to the crystalline forms of carbon their microstructure is quite complex, they are often porous and can contain other elements as impurities.

Briefly, non-graphitic carbons consist of graphene sheets that pile up to form stacks of a few nanometres in size. Different from graphite, where the graphenes pile up regularly (hexagonal, AB stacking or rhombohedral, ABC stacking), the graphenes in non-graphitic carbons are only more or less parallel packed upon each other (Fig. 3a and b). The graphenes can be embedded in an amorphous matrix and also be connected among each other. The size of the graphene stacks can be estimated by XRD (L$_a$ and L$_c$)[8] or Raman spectroscopy (L$_a$).[9] Due to their disorder, non-graphitic carbons usually contain a large number of slit-shaped micropores. Typical examples for non-graphitic carbons are activated carbons, carbon aerogels or carbon black.

Activated carbons are usually synthesized by heat treatment of organic matter in inert atmosphere (carbonization or pyrolysis). The use of natural precursors such as coal, wood or
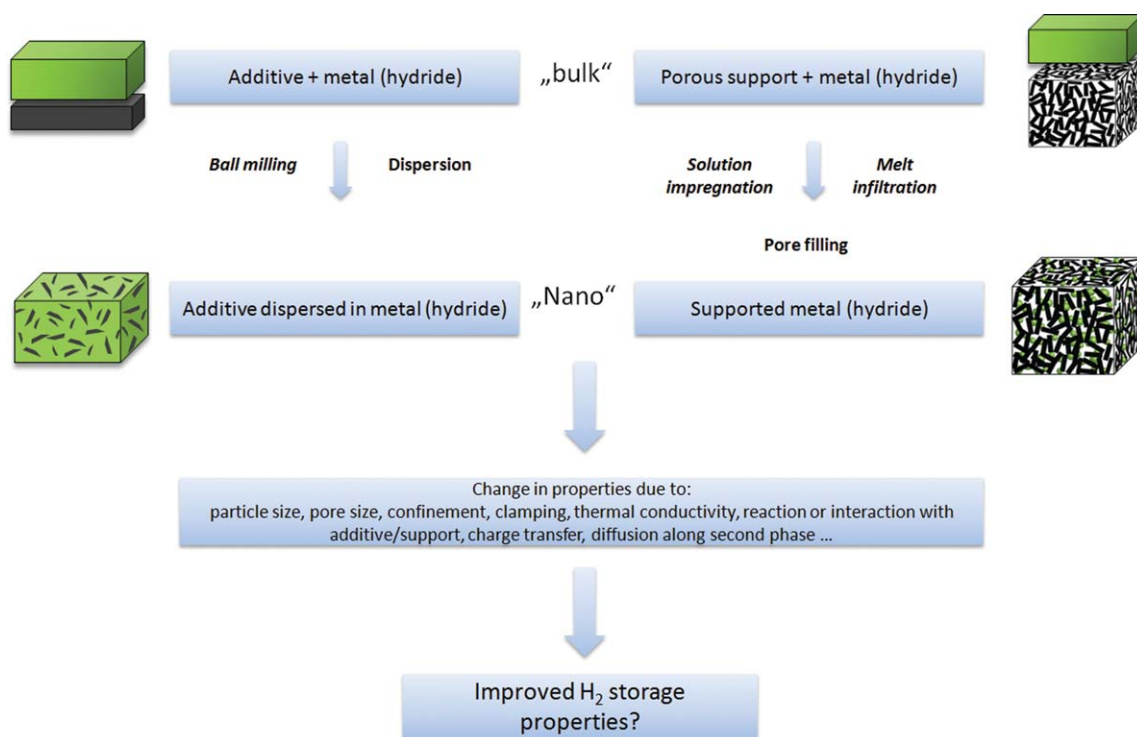
Fig. 2   The hydrogen storage properties of metal hydrides can be tailored by mixing with an additive (usually ball-milling) or by supporting on a porous material using solution impregnation or melt infiltration. The resulting nanocomposites exhibit different properties compared to the bulk metal hydrides.

coconut shell allows a low cost production and is the reason for their widespread use. The high surface area is obtained by activation processes such as steam activation. Typically, activated carbons are highly microporous ($d < 2$ nm) with a broad pore size distribution, and exhibit surface areas between 500 and 1200 m^2 g^{-1}.
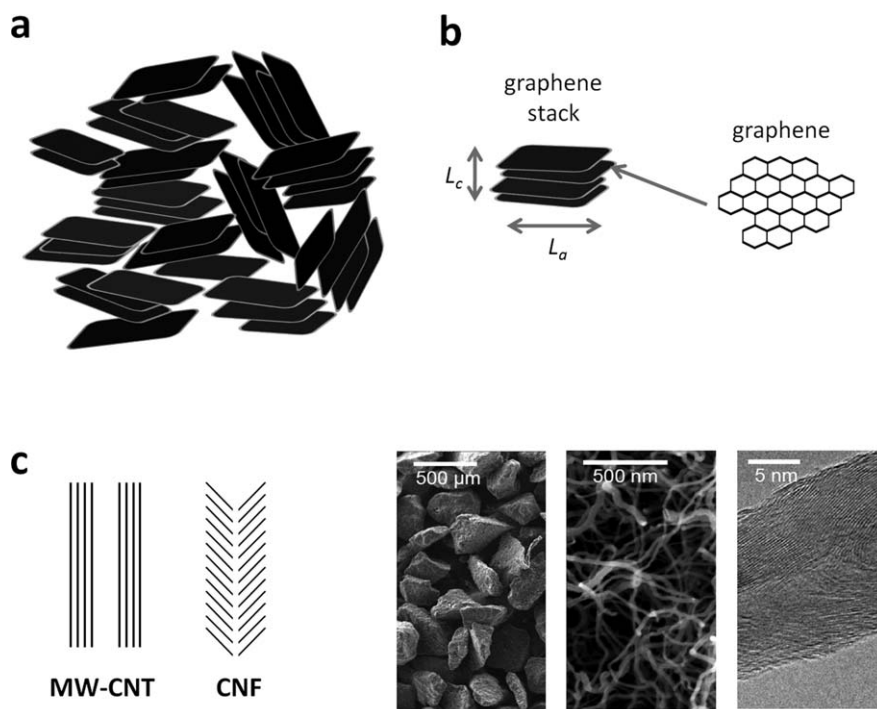

Fig. 3   (a) Sketch of the microstructure in turbostratic carbon materials. (b) Illustration of a single graphene stack. The dimensions are described by layer size L_a and stack height L_c. (c) *left:* Orientation of the graphenes in carbon nanotubes and nanofibers. *right:* SEM and TEM images of carbon nanofibers, reprinted by permission of the publisher (Taylor & Francis Group).

Carbon black consists of spherically shaped carbon nanoparticles and their fused aggregates, synthesized by incomplete combustion or thermal decomposition of gaseous/liquid hydrocarbons. Oils, natural gas or acetylene usually serve as feedstock. Carbon blacks can be synthesized with surface areas up to 1500 m^2 g^{-1} and are industrially used as reinforcing fillers, pigments or conducting agents, for example.[10,11]

Carbon aerogels (cryogels, xerogels) can be described as mesoporous ($d = 2–50$ nm) networks that are formed by loosely connected carbon nanoparticles. The mesopore volume of carbon aerogels can be quite large (>0.55 cm^3 g^{-1}). Carbon aerogels are synthesized by careful carbonization of organic aerogels (resorcinol/formaldehyde or phenol/furfural aerogels) under inert atmosphere and can be obtained in monolithic form. Depending on the synthesis parameters, the mesopore size can be adjusted. Carbon aerogels typically exhibit surface areas between 600 and 800 m^2 g^{-1} and a relatively large micropore volume.[12–15]

Carbon materials with monodisperse pores of a particular shape in the nanometre range are more difficult to realize, however, they are desired to study size effects. Ordered and disordered porous carbon materials with defined porosity can be synthesized using the templating method, also known as *nanocasting*. Thereto, a porous template (SiO_2 or zeolite) is first impregnated with a carbon precursor. After carbonization of the precursor and dissolution of the template, a porous carbon replica is obtained.[16] Depending on the template and carbon precursor, carbon replicas with different pore sizes can be synthesized, *e.g.* CMK-3 with ordered mesopores of 4.5 nm in diameter is a replica of SBA-15 (silica).[17,18] In another approach, silica nanoparticles are dispersed in the carbon precursor prior to carbonization. Also polymers have been used as porogen.[19]

Carbide derived carbons (CDCs) are microporous carbons with defined pore size and controllable pore volume and are synthesized by selective thermo-chemical etching of metal atoms from carbides.[20,21]

Carbon materials with medium high surface areas and very well defined structure are *carbon nanofibers* (CNFs) and *carbon nanotubes* (CNTs). CNFs and CNTs typically exhibit surface areas between 10 and 400 m^2 g^{-1} and diameters between 10 and 200 nm.[22,23] Both can be synthesized by the catalytic decomposition of carbon containing gases (*e.g.* CH_4, CO, C_2H_4), using small metal particles as the growth catalyst. An interesting feature is that their surfaces exhibit exclusively either the basal planes (CNT) or edge planes (CNF) of the graphenes. *Fullerenes* are another class of well defined carbon materials with spherical structure build of hexagonal and pentagonal rings. A diameter of 0.78 nm is reported for C_{60}, for example.[24,25]

Fig. 3 gives an overview of the structure of different carbon materials. A selection of carbon materials and their properties are summarized in Table 1.

3. Synthesis strategies

The most frequently used method to prepare carbon/metal hydride nanocomposites is *ball-milling*. Ball-milling reduces the particle/crystallite size of metal (hydrides)[26–31] down to around 20–30 nm and introduces many defects and amorphous areas that enhance diffusion processes. However, the "nanoeffect" is usually lost upon cycling due to crystal growth.[32,33] In ball-milling, carbon is used as an additive (typically 5–15 wt%) that is dispersed in the metal (hydride) phase during the milling process rather than a support. Many different carbon materials among CNTs, C_{60}, graphite, carbon blacks, activated carbons and ordered mesoporous carbons have been investigated and generally speaking all of them show positive effects on the hydrogen sorption properties. However, care has to be taken when interpreting the results, as ball-milling can destroy the carbon structure (amorphization)[34] and certain carbon materials contain classical catalysts as impurities. CNTs and CNFs can contain Ni, Co or Fe impurities, for example that can get into contact with the metal (hydride) phase due to destruction of the tubes upon ball-milling.[35,36] Also the ball mill vial or the (typically steel) balls are sources for contaminations.[37]

The main routes to prepare carbon supported metal hydrides are *solution impregnation* and *melt infiltration*. To be suitable as a support, the carbon material should exhibit (1) a high surface area, (2) an accessible pore system and (3) a large total porosity in order to allow high weight loadings of metal hydride. To study the size effects and interaction with the support, a defined pore size and surface are desirable.

In solution impregnation, a solution of the hydride or a precursor is used to infiltrate the porous carbon material. Then, the solvent is evaporated to leave finely dispersed nanoparticles on the support. This technique is well known from catalyst preparation and has the advantage that relatively small nanoparticles (<10 nm) of defined size can be prepared. A main drawback is that the synthesis involves a multi-step procedure and higher loadings of metal (hydride) can be often only obtained by multiple impregnation and drying, as for many compounds the solubility is low. Thus, concerning hydrogen storage materials, solution impregnation is an excellent technique to synthesize model systems; however, other methods are needed to synthesize larger quantities more cost-effective.

Melt infiltration allows the synthesis of higher weight loadings in a single step. Here, the metal or metal hydride is melted under

Table 1 Selection of carbon materials that can be used as additive or support for metal hydrides

	Surface area/m^2 g^{-1}	Predominant porosity	Purity	Price
Activated carbons	500–1200	Micro, (meso)	Poor	Low
Carbon aerogels	250–2000	Micro, meso, macro	High	High
Carbon black	10–400	Micro, meso	High	Low
Carbon nanotubes and fibers	100–400	Micro, meso	High-medium	High
Templated carbons (*e.g.* CMK-3)	200–1500	Meso, micro	High	Very high
Carbide derived carbons	1000–2000	Micro	High-medium	Very high

appropriate conditions. In case of wetting, *i.e.* the contact angle of the melt on the support is smaller 90°, the pores of the support are filled by capillary force. After cooling and solidification, the metal (hydride) is confined in the pores of the support. Ideally, the particle size is defined by the pore size of the support. In nanopores, the capillary pressure can be as high as 1000 bar, so the driving force for pore filling is very high. On the contrary, in the case of non-wetting (contact angle of the melt >90°), external pressure has to be applied to fill the pores of the support.[38]

4. Potential impact of the carbon supports/additives

Carbon materials exhibit certain properties that make them in combination with metal hydrides more suitable compared to other potential supports or additives. An important property is their relative chemical inertness, especially because light metal hydrides are chemically very reactive. However, some possible reactions/interactions with a carbon matrix do exist among the most important ones are *intercalation*, *carbide formation* and interactions with *terminating groups* or *defects*. In some cases, these interactions are beneficial to the hydrogen sorption properties of metal hydrides, in others they are unwanted. Also, the ability of carbon to efficiently conduct heat and the fast H_2 diffusion along the carbon phase can improve the hydrogen sorption properties.

Intercalation

A well known property of graphite (and non-graphitic carbon materials) is the ability to form lamellar intercalation compounds with many species, in particular alkali metals.[39–41] A technologically important graphite intercalation compound is LiC_6 which forms the negative electrode material in today's lithium ion batteries. The intercalation/deintercalation process is highly reversible and can allow thermodynamic tailoring of a metal (hydride) system. As the intercalation process is exothermic ($\Delta H = -13.9$ kJ mol^{-1} [Li] for LiC_6),[42] the metal phase is stabilized towards the hydride phase and consequently ΔH for the de-/hydrogenation reaction is reduced. This principle was recently demonstrated for the hydrogen release from NaH.[43] Also, ternary intercalation compounds of hydrogen/alkali metal/graphite are known.[44]

Carbide and methane formation

Carbide formation (Li_2C_2, Na_2C_2, CaC_2,...) is thermodynamically favored for certain light metals, however, they form only at higher temperatures due to kinetic limitations. Li_2C_2 formation starts at ~400 °C, for example. In principle, carbide formation is undesired, as the carbon structure is destroyed and metal hydride formation from the carbide phase is likely to be difficult. Some reports do exist on graphite/LiH nanocomposites,[45,46] and carbon/$LiBH_4$ nanocomposites[47] where hydrogen uptake and release involve the formation of Li_2C_2. However, it was found that CH_4 can form during cycling, *i.e.* the carbon content gradually decreases upon cycling.[45] Thermodynamically, methane formation is favorable for systems involving H_2 and C and can occur at elevated temperatures, especially when catalytic species are present. This can become relevant when the hydrogenation is conducted at high temperatures and high hydrogen pressures.[45]

Terminating groups, defects and contamination

Whether solution impregnation or melt infiltration is used as synthesis method, wetting of the support is crucial and can be adjusted by the surface chemistry of the carbon materials. As the edges of the graphenes need to be terminated, non-graphitic carbons contain a certain amount of other atoms, usually H, O and N that determine the surface energy and thus the interaction with other phases. Nature and concentration of the terminating species can vary depending on the carbon precursor, carbonization temperature or chemical post-treatment.[48–53] The terminating species also provide possible sites for chemical reactions with the metal (hydride) phase. Fig. 4 gives an overview over possible oxygen and nitrogen containing terminating groups at the edges of the graphenes. Ideally, CNTs and fullerenes exhibit no terminating groups and thus represent the purest form of carbon nanomaterials.

Also, structural defects within the graphene exist that might be catalytically active.[54–56] It is suggested that defects in the form of non-hexagonal rings can ease the dissociation of gas molecules.[57,58] For example, O_2 preferentially dissociates at vacancies in graphite.[59] If the same holds for the dissociation of H_2, structural defects in carbon materials would be a powerful tool to improve the hydrogen sorption properties of carbon supported metal hydrides.

The wetting properties and surface energies of the carbon support can be adjusted from hydrophobic "pure" carbon to hydrophilic carbon with hydroxyl terminating groups, for example. For graphite, a surface energy of 0.077 J m^{-2} was found for the basal planes (at 970 °C) whereas 4 J m^{-2} was found for the edge planes.[61] One could therefore expect that CNFs can be wetted easier than CNTs. On the other hand, light metals can irreversibly react with certain surface groups, leading to a loss in active material but facilitate wetting.

Common techniques to determine the amount and/or nature of surface groups are elemental analysis, titration methods, temperature programmed desorption/oxidation, X-ray photoelectron spectroscopy and infrared spectroscopy methods.[50–52,62–64] Carbon materials also often contain all sorts of impurities, especially when made from natural precursors such as biomass, oil or pitch and metals such as K, Fe, Ni, and Co[64] that might interact with the metal hydride phase or could act as catalyst.
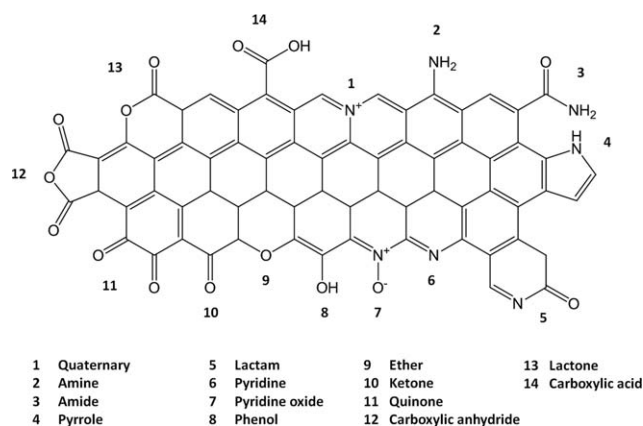

1	Quaternary	5	Lactam	9	Ether	13	Lactone
2	Amine	6	Pyridine	10	Ketone	14	Carboxylic acid
3	Amide	7	Pyridine oxide	11	Quinone		
4	Pyrrole	8	Phenol	12	Carboxylic anhydride		

Fig. 4 Possible oxygen and nitrogen species and terminating groups at the edge of a graphene (redrawn from ref. 60).

This journal is © The Royal Society of Chemistry 2011

J. Mater. Chem., 2011, **21**, 2417–2427 | 2421

H₂ diffusion promoter

Hydrogen diffusion through the bulk metal (hydride) phase is usually quite slow and often rate-limiting. In either case, *i.e.* metal hydride dispersed over a porous carbon structure, or carbon material dispersed in the metal hydride phase, fast hydrogen diffusion through or along the carbon phase could benefit the kinetics of hydrogen release and uptake.

Thermal conductivity

The ability of carbon to effectively conduct heat is an important advantage over other inorganic support materials as it enhances the heat exchange during de/rehydrogenation. The thermal conductivity of graphite is highly anisotropic and typically found to be around 12–175 W m^{-1} K^{-1}.[65] Even though the effective thermal conductivity depends on many parameters such as particle size, porosity, tank design, *etc.*, it was found that even small amounts of graphite significantly improve the heat conduction of metal hydride compacts. Kim *et al.* found a thermal conductivity of >3 W m^{-1} K^{-1} for compacts of LaNi$_5$ containing 2% graphite,[66] which is much higher than ~0.1 W m^{-1} K^{-1} that are typically found for metal hydride powders. Sanchez *et al.* found the thermal conductivity of metal hydride/graphite compacts to be higher compared to when aluminium foams were used as conducting agent.[67]

Dispersion of a catalyst

Carbon materials can also be used to incorporate additional catalysts to further improve the kinetics of hydrogen release and uptake. Ni and Co are well-known catalysts for the dissociation of hydrogen molecules and can easily be dispersed on the carbon support prior to the preparation of the carbon/hydride composite, for example.[68,69] Also CNTs and CNFs usually contain small amounts of Ni or Co nanoparticles that get distributed in the hydride phase during ball milling.[70]

5. Key results on MgH₂ and NaAlH₄

In the following, the beneficial effect of carbon on the hydrogen sorption properties is discussed for a conventional hydride (magnesium hydride—MgH$_2$) and a complex hydride (sodium alanate—NaAlH$_4$), as they are among the most studied hydrides and illustrative for many other systems. For studies on the effect of carbon on other hydrogen storage compounds such as NH$_3$BH$_3$, LiBH$_4$ or Li$_3$BN$_2$H$_8$ we refer to the relevant literature.[6]

Magnesium hydride—MgH₂

Magnesium hydride is extensively studied as hydrogen storage material due to its low cost and relatively high hydrogen content of 7.7 wt%. However, its application is hindered by the high stability of the hydride and the poor kinetics of de- and rehydrogenation. The large negative enthalpy of formation of $\Delta H = -75$ kJ mol^{-1} corresponds to an equilibrium temperature of ~300 °C at 1 bar H$_2$. Kinetic limitations lead to practical dehydrogenation temperatures above 400 °C for bulk MgH$_2$. A significant decrease in the thermodynamic stability is predicted for particle sizes smaller than ~1 to 2 nm.[71,72] As the synthesis of

particles smaller than 2 nm is very challenging, it is an important question whether confinement in a support could further decrease the stability of the hydride. Liang and Kung calculated a reduction of the enthalpy of formation by 50% for the confinement of MgH$_2$ clusters in (10, 10) CNTs of 1.2 nm in diameter, for example.[3]

So far, most research was devoted to ball-milling of Mg(H$_2$) with different carbon materials, among CNTs, C$_{60}$, graphite, activated carbons.[35,73–77] The effect of carbon as additive on the hydrogen release from ball-milled MgH$_2$ is illustrated in Fig. 5. Generally speaking, all carbons show positive effects on the hydrogen sorption properties, *i.e.* improved kinetics and cycle life, however, the exact mechanism is still a matter of debate.[70,77–80]

The addition of graphite to the milling process generally leads to a reduction in crystallite size, which shortens the diffusion paths. However, studies on Mg nanoparticles with similar size but either milled with graphite or without did not show the same kinetic behavior. It was therefore suggested that graphite prevents the formation of unwanted oxide layers during the ball-milling process that otherwise impede the H diffusion.[75] Among the different carbon materials tested, usually CNTs and CNFs show best performance. For example, the rates of hydrogen uptake and release of Mg milled with CNTs were found to be more than one order of magnitude higher than that of pure Mg.[81] It is suggested that added nanotubes act as channels for fast hydrogen diffusion. Accordingly, the catalytic effect decreases upon long milling times once the CNT structure gets destroyed.[82] The improved performance might be also due to a synergetic effect, as CNTs and CNFs contain metal impurities (Co and Ni) as effective hydrogenation/dehydrogenation catalysts.[35,69] On the other hand, investigations on MgH$_2$/CNTs composites indicate that the catalytic effect of metal impurities is lost during cycling and the improved cyclability is due to fact that CNTs also prevent particle growth.[77] Another explanation for the catalytic activity of carbon arises from DFT calculations on a Mg(0001) surface that includes subsurface carbon atoms.[83] The calculations suggest that subsurface carbon (which might be incorporated into the metal phase during ball-milling) only slightly affects the dissociation of H$_2$ at the Mg surface but it facilitates the diffusion of atomic hydrogen into the subsurface by lowering the transport activation barriers. A more detailed discussion on the kinetic effect of defined carbon nanostructures is given by Wu and Cheng.[85]

Imamura *et al.*[86] reported on the enhanced hydrogen absorption properties for supported Mg nanoparticles that were synthesized by solution impregnation of activated carbon (1040 m^2 g^{-1}) with magnesium dissolved in ammonia. Also carbon aerogels ($d_{pore} = 13$ nm) have been infiltrated with a solution of dibutylmagnesium (MgBu$_2$) in heptane. The supported MgH$_2$ nanoparticles were obtained by hydrogenation of MgBu$_2$ and exhibited dehydrogenation kinetics >5 times faster compared to the MgH$_2$ reference that was ball-milled with graphite.[87]

Supported magnesium nanoparticles of varying size were prepared using melt infiltration of porous carbons with different pore size.[84] Even though nanoparticles smaller than 2 nm can be synthesized with this approach, no thermodynamic effect on the hydrogen sorption properties is reported so far. However, improved kinetics and cyclability are reported, especially when adding small amounts of Ni as catalyst.[68,88] The wetting of
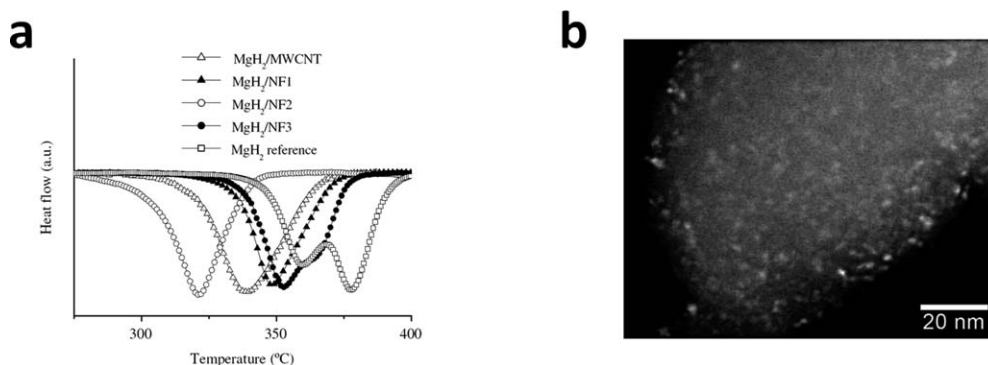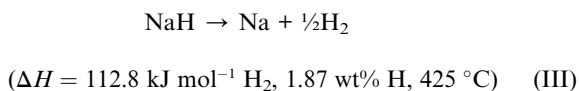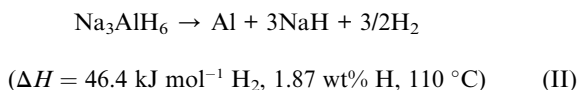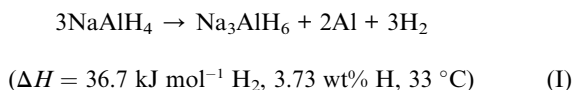
Fig. 5 (a) Hydrogen release from MgH$_2$ after ball milling for 2 h with (5 wt%) and without different carbon materials: (MWCNT) multi-walled carbon nanotubes and (NF1-3) carbon nanofibers with increasing surface area. (Data obtained with DSC, 5 °C min^{-1}, Ar flow.) Reprinted from ref. 35, with permission from Elsevier. (b) Dark-field TEM image of a nanoporous carbon after melt infiltration with 33 wt% Mg. The well dispersed Mg nanoparticles can be seen as bright spots. Reprinted from ref. 84. Copyright 2007 American Chemical Society.

magnesium is enhanced by distributing Ni or Cu metal nanoparticles on the carbon matrix before melt infiltration. Composites containing more than 80 wt% Mg can be prepared this way,[68] however, also crystalline Mg was found by XRD when exceeding weight loadings of approx. 15 wt%. Care has to be taken during preparation as magnesium has a comparably high vapor pressure and can easily oxidize at the infiltration temperature ($T_{m,Mg} = 650$ °C).

In summary, the kinetics of the MgH$_2$ system can be significantly enhanced by supporting it on carbon or by adding carbon materials during ball-milling. The cyclability is improved, as carbon reduces particle agglomeration and growth. Even though beneficial thermodynamic effects are predicted from theory,[3,71,72] no effect on the thermodynamics using carbon as additive or support has been reported in open literature so far. However, it is worth to note that a slight decrease in the thermodynamic stability by 2.84 kJ mol^{-1} was recently found for Mg nanoparticles of ~7 nm in size which were embedded in a LiCl matrix by ball-milling.[89]

Sodium alanate, NaAlH$_4$

NaAlH$_4$ is the most studied complex hydride, as it is one of the few compounds that combines viable thermodynamical properties[90] and a relatively high hydrogen storage capacity. Sodium alanate decomposes in three steps upon heating, releasing 7.4 wt% H$_2$ per NaAlH$_4$:

$$3NaAlH_4 \rightarrow Na_3AlH_6 + 2Al + 3H_2$$

$$(\Delta H = 36.7 \text{ kJ mol}^{-1} \text{ H}_2, 3.73 \text{ wt% H}, 33 \text{ °C}) \qquad (I)$$

$$Na_3AlH_6 \rightarrow Al + 3NaH + 3/2H_2$$

$$(\Delta H = 46.4 \text{ kJ mol}^{-1} \text{ H}_2, 1.87 \text{ wt% H}, 110 \text{ °C}) \qquad (II)$$

$$NaH \rightarrow Na + \frac{1}{2}H_2$$

$$(\Delta H = 112.8 \text{ kJ mol}^{-1} \text{ H}_2, 1.87 \text{ wt% H}, 425 \text{ °C}) \qquad (III)$$

Even though reactions (I) and (II) should occur at 33 °C and 110 °C under atmospheric hydrogen pressure the course of the

reactions is strongly kinetically hindered and substantial decomposition of bulk NaAlH$_4$ only starts after reaching the melting point ($T_m = 180$ °C). NaH reaches an equilibrium pressure of 1 bar H$_2$ only at 425 °C. Generally speaking, the challenges for reactions (I) and (II) are to use/find suitable catalysts, such as Ti[91,92] and to prevent phase segregation into larger domains of Al and NaH upon dehydrogenation that hampers the reversibility of the reactions. NaH decomposes at temperatures too high for practical use, unless the thermodynamics of reaction (III) could be significantly altered. As will be shown, all these challenges can be tackled by using carbon as support.

It was first noted in 2000 that NaAlH$_4$ ball-milled with carbon exhibits significantly improved hydrogen sorption properties compared to conventionally milled NaAlH$_4$.[27] Fig. 6a shows the decomposition of NaAlH$_4$ at 160 °C with and without 10 wt% carbon (the nature of the carbon was not further specified). The reaction rates of reactions (I) and (II) increased and improved rehydrogenation behavior was found.[78,93,94] Since then, several carbon materials have been tested. For graphite, it is suggested that its beneficial effect on the milling process might be due to a dual function, *i.e.* dry lubricant and micro-grinding agent as a result of carbide formation.[95]

It was also reported that significant improvements can be also obtained by simple mixing of NaAlH$_4$ with carbon materials.[43,96] Even for μm sized NaAlH$_4$ particles, a strong shift in the dehydrogenation maxima (reactions (I)–(III)) to lower temperatures was observed. In a study using 18 wt% CNT, C$_{60}$ and graphite dispersed in NaAlH$_4$, C$_{60}$ was identified as most active carbon modification, as it interfaced most of its surface to the NaAlH$_4$.[97] In the same work, the catalytic effect of carbon on the de- and rehydrogenation of NaAlH$_4$ was also explained with its electronegative nature. The bonds in NaAlH$_4$ are ionic between Na$^+$ and AlH$_4^-$ and covalent between Al and H. It is suggested that the presence of the electronegative carbon affects the ability of Na to donate the electron to AlH$_4$, therefore weakening the Al–H bonds and thus allowing easier hydrogen release and uptake, although it remains a question whether electronic effects could extend beyond 1–2 nm in ionic materials.

Solution impregnation was used to synthesize NaAlH$_4$ nanoparticles on CNF (130 m^2 g^{-1}) using THF as solvent.[7,98] Nanoparticles of different size were prepared by varying the synthesis
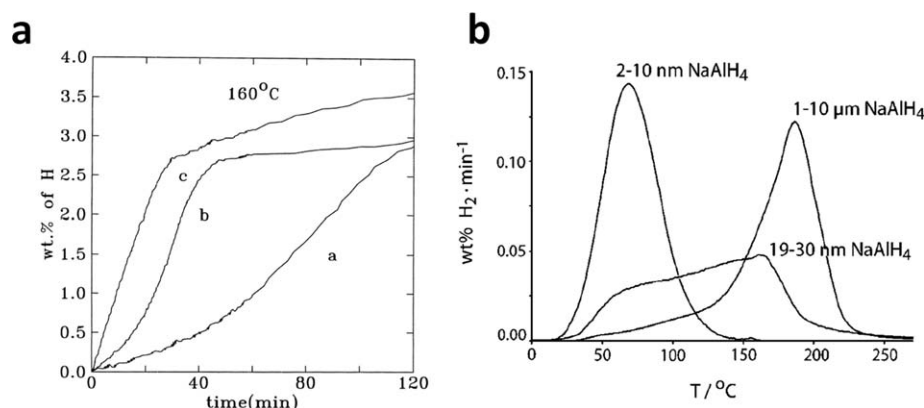
Fig. 6 Kinetic effects on the hydrogen release from NaAlH$_4$: (a) Decomposition of ball-milled NaAlH$_4$ at 160 °C. a 1st Decomposition without carbon. b and c 1st and 2nd decomposition with 10 wt% carbon. Reprinted from ref. 27 with permission from Elsevier. (b) Hydrogen release (TPD, 5 °C min^{-1}, Ar flow) from NaAlH$_4$ particles of different sizes deposited on carbon nanofibers (CNF). Reprinted with permission from ref. 7. Copyright 2008 American Chemical Society.

conditions and a quantitative relation between particle size and the activation energy for H$_2$ release was found. For the smallest particles (d = 2–10 nm, 2 wt% NaAlH$_4$), an activation energy of 58 kJ mol^{-1} was found, *i.e.* much lower than the activation energy for μm-sized particles (116 kJ mol^{-1}) or Ti catalyzed NaAlH$_4$. The maximum hydrogen release rate (under Ar) was found to be around 60 °C compared to 180 °C for bulk NaAlH$_4$ (Fig. 6b).

NaAlH$_4$ melt infiltration has to be conducted in an autoclave, as the liquid NaAlH$_4$ phase ($T_{m,NaAlH_4}$ = 180 °C) is only stable at hydrogen pressures above 130 bar.[91] Carbon aerogels,[100,101] high surface area carbon[102] (500 m^2 g^{-1}) and activated carbon fibers[99] (1815 m^2 g^{-1}) were tested for this purpose. In a detailed study on the melt infiltration process, it was found that the pore filling is a relatively fast process and that the confinement in the carbon nanopores (2–3 nm) yields a NaAlH$_4$ phase without long range crystallinity.[103] Similar to earlier works, only Al but no NaH or Na diffraction lines was found by XRD after dehydrogenation.[7,43] This indicates a higher dispersion of Na(H) compared to Al, which might be due to a stronger interaction of Na(H) with the carbon support. Enhanced kinetics and improved reversibility compared to bulk NaAlH$_4$ were reported by all groups. However, of greater importance is the effect on the thermodynamic properties: two groups reported a change in the thermodynamic properties of the NaAlH$_4$ system due to the nanosize and confinement in the porous carbon matrix.[99,102,104] Both groups used carbons of high purity, *i.e.* negligible metal content and with pores in the micro- and mesopore range. Fig. 7 shows the pressure–composition-isotherms (PCIs) of CeCl$_3$ catalyzed bulk NaAlH$_4$ in comparison with nanoconfined NaAlH$_4$. Interestingly, the typical two step behavior (reactions (I) and (II)) is found to be absent for the nanoconfined NaAlH$_4$. Instead, the PCI of the nanoconfined NaAlH$_4$ shows more the behavior of a solid solution. Also it was found that during rehydrogenation in the stability region of the Na$_3$AlH$_6$, NaAlH$_4$ forms instead directly from NaH, Al and 3/2H$_2$. The absence of Na$_3$AlH$_6$ in the carbon nanoconfinement was confirmed by NMR measurements.[102] The results point on an interesting fact: whereas MgH$_2$ is predicted to thermodynamically destabilize upon nanosizing and confinement, NaAlH$_4$ seems to be stabilized by confinement

in a nanoporous carbon support. However, further experimental and theoretical work is important to determine how exactly Na$_3$AlH$_6$ and NaAlH$_4$ are thermodynamically altered by the confinement and close contact to the carbon matrix.[105]

The kinetics and thermodynamics of reaction (III) also change for NaH being in contact with a porous carbon material. Even for bare mixtures of NaH and carbon, the dehydrogenation
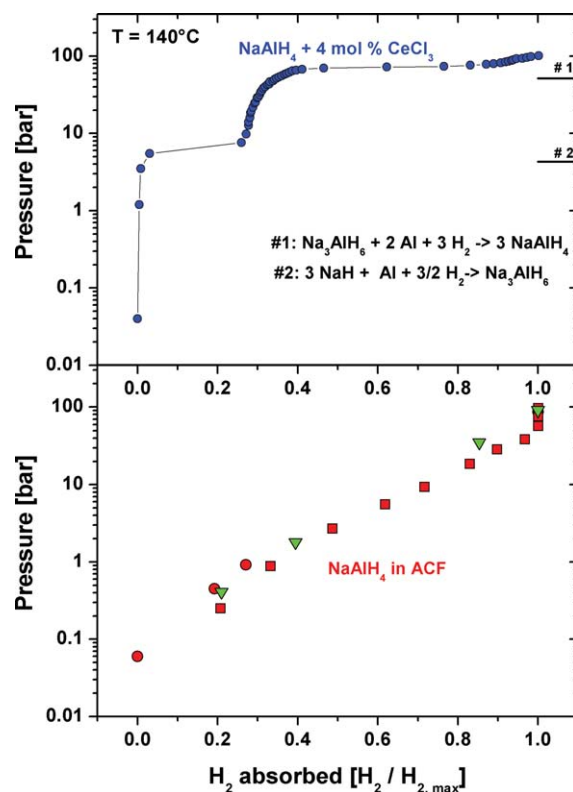

Fig. 7 Thermodynamic effects on carbon supported NaAlH$_4$: isotherm of CeCl$_3$ catalyzed NaAlH$_4$ showing the equilibria conditions of reactions (I) and (II), and isotherm of NaAlH$_4$ after melt infiltration of activated carbon fibers (ACF, 48 wt% NaAlH$_4$). The isotherms are normalized on the maximum hydrogen capacity obtained for the samples. Courtesy: W. Lohstroh, adapted from ref. 99.

temperatures under Ar can decrease by more than 100 °C. Upon heating of NaH/carbon mixtures and dehydrogenation, liquid Na ($T_{m,Na}$ = 97.7 °C) readily infiltrates the porous carbon structure. Fig. 8a shows a series of XRD patterns starting from the NaH/carbon mixture. After dehydrogenation (melt infiltration) one can see a broad Na diffraction line indicative for nanosized crystallites and a clear shift of the (002) diffraction line around 30° towards lower scattering angles due to intercalation of the carbon matrix.

Deintercalation occurs upon gradual rehydrogenation. As a result of intercalation and interaction with the carbon matrix, the equilibrium hydrogen pressure of carbon supported NaH is partially shifted to higher values with hydrogen release under

1 bar H_2 starting from around 225 °C, which is 200 °C below than what is expected for bulk NaH (Fig. 8b).[43]

In summary, the NaAlH$_4$–carbon system is an excellent example of how strongly a carbon material can influence both kinetics of hydrogen release and uptake, as well as the thermodynamics, of a hydrogen storage material. Hydrogen release from NaAlH$_4$ and NaH is even facilitated by bare mixing with carbon materials. A change in thermodynamics occurs for NaAlH$_4$ and NaH confined in the pores of micro/mesoporous carbons.

6. Conclusion

In this review we have discussed the impact of carbon materials on the hydrogen storage properties of metal hydrides. Nanosizing and nanoconfining are promising routes to meet the kinetic and thermodynamic requirements necessary for practical application and both routes are accessible by using carbon materials as support or additive. Additionally carbon materials are light and low in cost, which makes them an ideal match for the preparation of metal hydrides based nanocomposites.

In general, carbon materials act as effective catalysts and improve the reversibility of the de- and rehydrogenation reaction, as growth of the metal hydride nanoparticles and crystallites is hindered upon cycling. As carbon materials are not classical catalysts, their strong effect on the kinetics is still a matter of debate probably owing to their complex microstructure. Especially terminating groups that include heteroatoms such as H, N or O or intrinsic defects might play an important role. Further insight in the catalytic effect of carbon on metal hydrides might be therefore gained by including heteroatoms or defects in theoretical model systems. Many carbon materials often also contain metallic impurities that can further improve the kinetics. This synergetic effect was found for ball-milled MgH$_2$/carbon nanocomposites, for example. Surprisingly, enhanced hydrogen release is also found for bare mixtures of micrometre sized carbon particles with NaAlH$_4$ or NaH, indicating that not only nanoeffects are responsible for the kinetic improvements in this system but also the carbon phase itself has an important role.

As an important point, it was shown that also the thermodynamic properties can be altered by supporting metal hydrides on a carbon support. For the NaAlH$_4$ system this change is two-fold. Whereas NaAlH$_4$ seems to be stabilized by the nanoconfinement, NaH is destabilized (at least partly due to intercalation effects). The impact on the thermodynamics is found for confinement in pores below a few nanometres size. Thus carbon materials with large pore volumes in the micro- and mesopore range are desirable to allow high weight loadings of the hydride. Further information on the size effect might be obtained by using ordered mesoporous and carbide derived carbons as support. However, it will remain a challenge to separate the effects of particle size, confinement, surface chemistry, *etc.*

In summary it is clearly demonstrated that the use of carbon materials offers many opportunities in tailoring the properties of metal hydrides. As their porosity and surface chemistry can be adjusted in a broad range, their use as support thus shows great potential for further improvements in hydrogen storage applications.
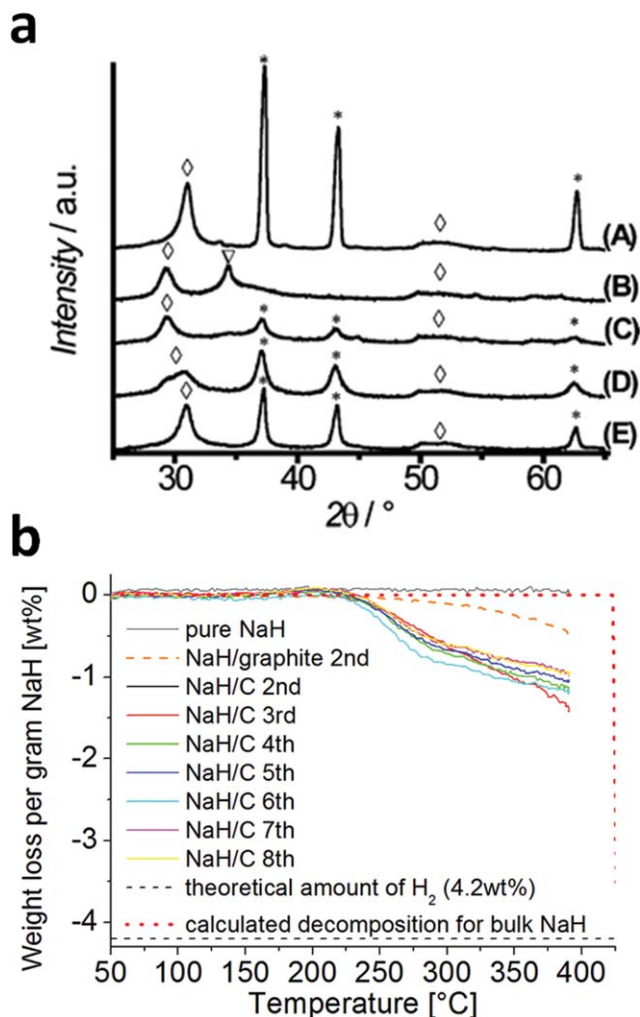

Fig. 8 Thermodynamic effects on carbon supported NaH: (a) XRD patterns of samples containing 33 wt% NaH on carbon. (A) Physical mixture of NaH and carbon for comparison. (B) After Na melt infiltration: intercalation leads to a shift of the (002) carbon diffraction line around 30° towards lower scattering angles. (C–E) Deintercalation upon gradual rehydrogenation of Na. ◇ = carbon, * = NaH, and ▽ = Na. (b) Hydrogen release from the nanocomposite (NaH/C) under atmospheric hydrogen pressure. Numbers indicate the cycle. The decomposition temperature of crystalline NaH is indicated for comparison.[43] Reproduced with permission of The Royal Society of Chemistry.

References

1 L. Schlapbach and A. Zuttel, *Nature*, 2001, **414**, 353–358.
2 Targets for Onboard Hydrogen Storage Systems for Light-Duty Vehicles, http://www1.eere.energy.gov/hydrogenandfuelcells/storage/pdfs/targets_onboard_hydro_storage_explanation.pdf.
3 J. J. Liang and W. C. P. Kung, *J. Phys. Chem. B*, 2005, **109**, 17837–17841.
4 V. Berube, G. Chen and M. S. Dresselhaus, *Int. J. Hydrogen Energy*, 2008, **33**, 4122–4131.
5 V. Berube, G. Radtke, M. Dresselhaus and G. Chen, *Int. J. Energy Res.*, 2007, **31**, 637–663.
6 P. E. de Jongh and P. Adelhelm, in *Handbook of Hydrogen Storage*, ed. M. Hirscher, Wiley-VCH, Weinheim, 2010.
7 C. P. Balde, B. P. C. Hereijgers, J. H. Bitter and K. P. de Jong, *J. Am. Chem. Soc.*, 2008, **130**, 6761–6765.
8 N. Iwashita, C. R. Park, H. Fujimoto, M. Shiraishi and M. Inagaki, *Carbon*, 2004, **42**, 701–714.
9 A. C. Ferrari and J. Robertson, *Phys. Rev. B: Condens. Matter Mater. Phys.*, 2000, **61**, 14095–14107.
10 J.-B. Donnet, *Carbon Black—Science and Technology*, Dekker, New York, 1993.
11 A. D. McNaught and A. Wilkinson, in *Compendium of Chemical Terminology*, Blackwell Scientific Publications, Oxford, 1997.
12 N. Husing and U. Schubert, *Angew. Chem., Int. Ed.*, 1998, **37**, 23–45.
13 N. Job, A. Théry, R. Pirard, J. Marien, L. Kocon, J.-N. Rouzaud, F. Béguin and J.-P. Pirard, *Carbon*, 2005, **43**, 2481–2494.
14 A. C. Pierre and G. M. Pajonk, *Chem. Rev.*, 2002, **102**, 4243–4265.
15 G. Reichenauer, A. Emmerling, J. Fricke and R. W. Pekala, *J. Non-Cryst. Solids*, 1998, **225**, 210–214.
16 R. Ryoo, S. H. Joo and S. Jun, *J. Phys. Chem. B*, 1999, **103**, 7743–7746.
17 S. Jun, S. H. Joo, R. Ryoo, M. Kruk, M. Jaroniec, Z. Liu, T. Ohsuna and O. Terasaki, *J. Am. Chem. Soc.*, 2000, **122**, 10712–10713.
18 R. Ryoo, S. H. Joo, M. Kruk and M. Jaroniec, *Adv. Mater.*, 2001, **13**, 677–681.
19 J. Lee, J. Kim and T. Hyeon, *Adv. Mater.*, 2006, **18**, 2073–2094.
20 Y. Gogotsi, A. Nikitin, H. H. Ye, W. Zhou, J. E. Fischer, Y. Bo, H. C. Foley and M. W. Barsoum, *Nat. Mater.*, 2003, **2**, 591–594.
21 Y. G. Gogotsi and M. Yoshimura, *Nature*, 1994, **367**, 628–630.
22 T. J. Barton, L. M. Bull, W. G. Klemperer, D. A. Loy, B. McEnaney, M. Misono, P. A. Monson, G. Pez, G. W. Scherer, J. C. Vartuli and O. M. Yaghi, *Chem. Mater.*, 1999, **11**, 2633–2656.
23 K. P. de Jong and J. W. Geus, *Catal. Rev. Sci. Eng.*, 2000, **42**, 481–510.
24 D. M. Guldi, A. Rahman, V. Sgobba and C. Ehli, *Chem. Soc. Rev.*, 2006, **35**, 471–487.
25 R. Taylor and D. R. M. Walton, *Nature*, 1993, **363**, 685–693.
26 A. Zaluska, L. Zaluski and J. O. Strom-Olsen, *J. Alloys Compd.*, 1999, **288**, 217–225.
27 A. Zaluska, L. Zaluski and J. O. Strom-Olsen, *J. Alloys Compd.*, 2000, **298**, 125–134.
28 J. Huot, G. Liang and R. Schulz, *Appl. Phys. A: Mater. Sci. Process.*, 2001, **72**, 187–195.
29 M. Fichtner, *Adv. Eng. Mater.*, 2005, **7**, 443–455.
30 M. U. Niemann, S. S. Srinivasan, A. R. Phani, A. Kumar, D. Y. Goswami and E. K. Stefanakos, *J. Nanomater.*, 2008, DOI: 10.1155/2008/950967.
31 K. F. Aguey-Zinsou and J. R. Ares-Fernández, *Energy Environ. Sci.*, 2010, **3**, 526–543.
32 Z. Dehouche, T. Klassen, W. Oelerich, J. Goyette, T. K. Bose and R. Schulz, *J. Alloys Compd.*, 2002, **347**, 319–323.
33 O. Friedrichs, F. Aguey-Zinsou, J. R. A. Fernandez, J. C. Sanchez-Lopez, A. Justo, T. Klassen, R. Bormann and A. Fernandez, *Acta Mater.*, 2006, **54**, 105–110.
34 N. Pierard, A. Fonseca, J. F. Colomer, C. Bossuot, J. M. Benoit, G. Van Tendeloo, J. P. Pirard and J. B. Nagy, *Carbon*, 2004, **42**, 1691–1697.
35 M. A. Lillo-Rodenas, Z. X. Guo, K. F. Aguey-Zinsou, D. Cazorla-Amoros and A. Linares-Solano, *Carbon*, 2008, **46**, 126–137.
36 Z. Z. Fang, X. D. Kang, P. Wang and H. M. Cheng, *J. Phys. Chem. C*, 2008, **112**, 17023–17029.
37 V. P. Balema, V. K. Pecharsky and K. W. Dennis, *J. Alloys Compd.*, 2000, **313**, 69–74.
38 T. Etter, A. Papakyriacou, P. Schulz and P. J. Uggowitzer, *Carbon*, 2003, **41**, 1017–1024.
39 M. S. Dresselhaus and G. Dresselhaus, *Adv. Phys.*, 2002, **51**, 1–186.
40 M. Noel and V. Suryanarayanan, *J. Power Sources*, 2002, **111**, 193–209.
41 H. Selig and L. B. Ebert, in *Advances in Inorganic Chemistry and Radiochemistry*, ed. H. J. Emeleus and A. G. Sharpe, Academic press, Inc., 1980, pp. 281–327.
42 V. V. Avdeev, A. P. Savchenkova, L. A. Monyakina, I. V. Nikolskaya and A. V. Khvostov, *J. Phys. Chem. Solids*, 1996, **57**, 947–949.
43 P. Adelhelm, K. P. de Jong and P. E. de Jongh, *Chem. Commun.*, 2009, 6261–6263.
44 T. Enoki, S. Miyajima, M. Sano and H. Inokuchi, *J. Mater. Res.*, 1990, **5**, 435–466.
45 H. Miyaoka, T. Ichikawa and Y. Kojima, *Nanotechnology*, 2009, **20**, 204021.
46 H. Miyaoka, K. Itoh, T. Fukunaga, T. Ichikawa, Y. Kojima and H. Fuji, *J. Appl. Phys.*, 2008, **104**, 053511.
47 X. B. Yu, Z. Wu, Q. R. Chen, Z. L. Li, B. C. Weng and T. S. Huang, *Appl. Phys. Lett.*, 2007, **90**, 034106.
48 H. P. Boehm, W. Heck, R. Sappok and E. Diehl, *Angew. Chem., Int. Ed. Engl.*, 1964, **3**, 669–677.
49 R. J. J. Jansen and H. van Bekkum, *Carbon*, 1994, **32**, 1507–1516.
50 R. J. J. Jansen and H. van Bekkum, *Carbon*, 1995, **33**, 1021–1027.
51 F. Rodriguez-Reinoso, *Carbon*, 1998, **36**, 159–175.
52 J. L. Figueiredo, M. F. R. Pereira, M. M. A. Freitas and J. J. M. Orfao, *Carbon*, 1999, **37**, 1379–1389.
53 H. Q. Jiang, F. Chen, M. G. Lagally and F. S. Denes, *Langmuir*, 2010, **26**, 1991–1995.
54 Q. H. Yang, W. H. Xu, A. Tomita and T. Kyotani, *Chem. Mater.*, 2005, **17**, 2940–2945.
55 F. Jaouen, M. Lefevre, J. P. Dodelet and M. Cai, *J. Phys. Chem. B*, 2006, **110**, 5553–5558.
56 M. Terrones, A. G. Souza and A. M. Rao, in *Carbon Nanotubes*, Springer-Verlag, Berlin, 2008, pp. 531–566.
57 D. S. Su, J. Zhang, B. Frank, A. Thomas, X. C. Wang, J. Paraknowitsch and R. Schlogl, *ChemSusChem*, 2010, **3**, 169–180.
58 J. M. Carlsson and M. Scheffler, *Phys. Rev. Lett.*, 2006, **96**, 046806.
59 J. I. Paredes, A. Martinez-Alonso and J. M. D. Tascon, *Carbon*, 2000, **38**, 1183–1197.
60 R. Arrigo, PhD thesis, *Nitrogen Functionalization of CNFs and Application in Heterogeneous Catalysis*, Technical University Berlin, Berlin, 2009.
61 T. W. Ebbesen, *Carbon Nanotubes: Preparation and Properties*, CRC Press, Inc., Boca Raton, 1996.
62 H. P. Boehm, *Carbon*, 2002, **40**, 145–149.
63 H. Aso, K. Matsuoka and A. Tomita, *Abstr. Pap. Am. Chem. Soc.*, 2003, **225**, 009-ENVR.
64 J. P. Tessonnier, D. Rosenthal, T. W. Hansen, C. Hess, M. E. Schuster, R. Blume, F. Girgsdies, N. Pfander, O. Timpe, D. S. Su and R. Schlogl, *Carbon*, 2009, **47**, 1779–1798.
65 F. Kohlrausch, *Praktische Physik*, B.G. Teubner, Stuttgart, 1986, vol. 3.
66 K. J. Kim, B. Montoya, A. Razani and K. H. Lee, *Int. J. Hydrogen Energy*, 2001, **26**, 609–613.
67 A. R. Sanchez, H. P. Klein and M. Groll, *Int. J. Hydrogen Energy*, 2003, **28**, 515–527.
68 R. Bogerd, P. Adelhelm, J. H. Meeldijk, K. P. de Jong and P. E. de Jongh, *Nanotechnology*, 2009, **20**, 204019.
69 M. A. Lio-Rodenas, K. F. Aguey-Zinsou, D. Cazorla-Amoros, A. Linares-Solano and Z. X. Guo, *J. Phys. Chem. C*, 2008, **112**, 5984–5992.
70 C. Z. Wu, P. Wang, X. D. Yao, C. Liu, D. M. Chen, G. Q. Lu and H. M. Cheng, *J. Phys. Chem. B*, 2005, **109**, 22217–22221.
71 S. Cheung, W. Q. Deng, A. C. T. van Duin and W. A. Goddard, *J. Phys. Chem. A*, 2005, **109**, 851–859.
72 R. W. P. Wagemans, J. H. van Lenthe, P. E. de Jongh, A. J. van Dillen and K. P. de Jong, *J. Am. Chem. Soc.*, 2005, **127**, 16675–16680.
73 S. Nohara, H. Inoue, Y. Fukumoto and C. Iwakura, *J. Alloys Compd.*, 1997, **252**, L16–L18.
74 S. Bouaricha, J. P. Dodelet and D. Guay, *J. Mater. Res.*, 2001, **16**, 2893–2905.

75 S. Bouaricha, J. P. Dodelet, D. Guay, J. Huot and R. Schulz, *J. Alloys Compd.*, 2001, **325**, 245–251.
76 J. L. Bobet, B. Chevalier, M. Y. Song and B. Darriet, *J. Alloys Compd.*, 2003, **356**, 570–574.
77 B. S. Amirkhiz, M. Danaie, M. Barnes, B. Simard and D. Mitlin, *J. Phys. Chem. C*, 2010, **114**, 3265–3275.
78 B. S. Amirkhiz, M. Danaie and D. Mitlin, *Nanotechnology*, 2009, **20**, 204016.
79 X. D. Yao, C. Z. Wu, A. J. Du, G. Q. Lu, H. M. Cheng, S. C. Smith, J. Zou and Y. H. He, *J. Phys. Chem. B*, 2006, **110**, 11697–11703.
80 X. D. Yao, C. Z. Wu, A. J. Du, J. Zou, Z. H. Zhu, P. Wang, H. M. Cheng, S. Smith and G. Q. Lu, *J. Am. Chem. Soc.*, 2007, **129**, 15650–15654.
81 C. Z. Wu, P. Wang, X. Yao, C. Liu, D. M. Chen, G. Q. Lu and H. M. Cheng, *J. Alloys Compd.*, 2006, **414**, 259–264.
82 C. Z. Wu, P. Wang, X. Yao, C. Liu, D. M. Chen, G. Q. Lu and H. M. Cheng, *J. Alloys Compd.*, 2006, **420**, 278–282.
83 A. J. Du, S. C. Smith, X. D. Yao and G. Q. Lu, *J. Phys. Chem. B*, 2006, **110**, 1814–1819.
84 P. E. de Jongh, R. W. P. Wagemans, T. M. Eggenhuisen, B. S. Dauvillier, P. B. Radstake, J. D. Meeldijk, J. W. Geus and K. P. de Jong, *Chem. Mater.*, 2007, **19**, 6052–6057.
85 C. Z. Wu and H. M. Cheng, *J. Mater. Chem.*, 2010, **20**, 5390–5400.
86 H. Imamura, Y. Usui and M. Takashima, *J. Less Common Met.*, 1991, **175**, 171–176.
87 S. Zhang, A. F. Gross, S. L. Van Atta, M. Lopez, P. Liu, C. C. Ahn, J. J. Vajo and C. M. Jensen, *Nanotechnology*, 2009, **20**, 204027.
88 A. F. Gross, C. C. Ahn, S. L. Van Atta, P. Liu and J. J. Vajo, *Nanotechnology*, 2009, **20**, 204005.
89 M. Paskevicius, D. A. Sheppard and C. E. Buckley, *J. Am. Chem. Soc.*, 2010, **132**, 5077–5083.
90 B. M. Lee, J. W. Jang, J. H. Shim, Y. W. Cho and B. J. Lee, *J. Alloys Compd.*, 2006, **424**, 370–375.
91 B. Bogdanovic, R. A. Brand, A. Marjanovic, M. Schwickardi and J. Tolle, *J. Alloys Compd.*, 2000, **302**, 36–58.
92 B. Bogdanovic and M. Schwickardi, *J. Alloys Compd.*, 1997, **253**, 1–9.
93 Z. Dehouche, L. Lafi, N. Grimard, J. Goyette and R. Chahine, *Nanotechnology*, 2005, **16**, 402–409.
94 J. Wang, A. D. Ebner and J. A. Ritter, *J. Phys. Chem. B*, 2006, **110**, 17353–17358.
95 J. Wang, A. D. Ebner, T. Prozorov, R. Zidan and J. A. Ritter, *J. Alloys Compd.*, 2005, **395**, 252–262.
96 C. Cento, P. Gislon, M. Bilgili, A. Masci, Q. Zheng and P. P. Prosini, *J. Alloys Compd.*, 2007, **437**, 360–366.
97 P. A. Berseth, A. G. Harter, R. Zidan, A. Blomqvist, C. M. Araujo, R. H. Scheicher, R. Ahuja and P. Jena, *Nano Lett.*, 2009, **9**, 1501–1505.
98 C. P. Balde, B. P. C. Hereijgers, J. H. Bitter and K. P. de Jong, *Angew. Chem., Int. Ed.*, 2006, **45**, 3501–3503.
99 W. Lohstroh, A. Roth, H. Hahn and M. Fichtner, *ChemPhysChem*, 2010, **11**, 789–792.
100 F. Schueth, B. Bogdanovic and T. Akira, WO/2005/014469, 2004.
101 R. D. Stephens, A. F. Gross, S. L. Van Atta, J. J. Vajo and F. E. Pinkerton, *Nanotechnology*, 2009, **20**, 204018.
102 J. B. Gao, P. Adelhelm, M. H. W. Verkuijlen, C. Rongeat, M. Herrich, P. J. M. van Bentum, O. Gutfleisch, A. P. M. Kentgens, K. P. de Jong and P. E. de Jongh, *J. Phys. Chem. C*, 2010, **114**, 4675–4682.
103 P. Adelhelm, J. B. Gao, M. H. W. Verkuijlen, C. Rongeat, M. Herrich, P. J. M. van Bentum, O. Gutfleisch, A. P. M. Kentgens, K. P. de Jong and P. E. de Jongh, *Chem. Mater.*, 2010, **22**, 2233–2238.
104 M. H. W. Verkuijlen, J. B. Gao, P. Adelhelm, P. J. N. van Bentum, P. E. de Jongh and A. P. M. Kentgens, *J. Phys. Chem. C*, 2010, **114**, 4683–4692.
105 T. Mueller and G. Ceder, *ACS Nano*, 2010, DOI: 10.1021/nn101224j.

This journal is © The Royal Society of Chemistry 2011

J. Mater. Chem., 2011, **21**, 2417–2427 | 2427